TRB

TRANSPORTATION RESEARCH RECORD

Journal of the Transportation Research Board, No. 2068

Pavement Monitoring, Evaluation, and Data Storage; Strength and Deformation Characteristics; and Surface Properties–Vehicle Interaction 2008

A Peer-Reviewed Publication

TRANSPORTATION RESEARCH BOARD
OF THE NATIONAL ACADEMIES

Washington, D.C.
2008

www.TRB.org

Prediction Models for Transverse Cracking of Jointed Concrete Pavements

Development with Long-Term Pavement Performance Database

Hsiang-Wei Ker, Ying-Haur Lee, and Chia-Huei Lin

The main objective of this study was to develop improved prediction models for transverse cracking of jointed concrete pavements with the Long-Term Pavement Performance database. The retrieval, preparation, and cleaning of the database were carefully handled with a systematic and automatic approach. The prediction accuracy of the existing prediction models implemented in the recommended *Mechanistic–Empirical Pavement Design Guide* (NCHRP Project 1-37A) was found to be inadequate. Exploratory data analysis indicated that the normality assumption with random errors and constant variance by using conventional regression techniques might not be appropriate for this study. Therefore, several modern regression techniques, including the generalized linear model and the generalized additive model, along with the assumption of Poisson distribution, were adopted for the modeling process. The resulting mechanistic–empirical model included several variables—such as pavement age, yearly equivalent single-axle loads (ESALs), accumulated ESALs, annual precipitation, freeze–thaw cycle, annual temperature range, stress ratio, and percent steel—for the prediction of transverse cracking. The goodness of fit was further examined through significant testing and various sensitivity analyses of pertinent explanatory parameters. The tentatively proposed predictive models appeared to agree reasonably with the pavement performance data, although their further enhancements are possible and recommended.

Performance predictive models have been used in various pavement design, evaluation, rehabilitation, and network management activities. Transverse cracking is one of the major distress types for jointed concrete pavements and is primarily caused by accumulated traffic loads and environmental effects. Extensive research has been conducted to predict the occurrence of this distress type by using various empirical and mechanistic–empirical approaches.

Conventional predictive models usually correlate transverse cracking to accumulated traffic, fatigue damage, environmental effects, and several other design parameters (*1–3*). As pavement design evolves from traditional empirically based methods toward mechanistic–empirical, the concept of the equivalent single-axle load (ESAL) used for traffic-load estimation is no longer recommended in the current *Mechanistic–Empirical Pavement Design Guide* (MEPDG) (NCHRP Project 1-37A) (*4*). The success of the new design guide considerably depends upon the accuracy of pavement performance predictions. Thus, this study first investigates its goodness of fit and strives to develop improved transverse-cracking prediction models for jointed concrete pavements by using the Long-Term Pavement Performance (LTPP) database (www.datapave.com or LTPP DataPave Online) (*5–7*).

REVIEW OF EXISTING MECHANISTIC–EMPIRICAL PREDICTION MODELS

NCHRP Project 1-19 (*1*) was conducted with the primary objective of developing a system for statewide and nationwide evaluation of concrete pavement performance. A total of 410 jointed plain concrete pavement (JPCP) and jointed reinforced concrete pavement (JRCP) sections representing 1,297 mi of concrete pavement were collected from six states distributed in various climatic regions, including Illinois, Georgia, Utah, Minnesota, Louisiana, and California. Eight additional JRCP pavement sections from Nebraska were also included in this database. The combined data represented about 6% of the total Interstate highway concrete pavements in the continental United States. Several combinations of multiple regression, stepwise regression, and nonlinear regression techniques were used to develop various pavement performance prediction models by using the SPSS statistical package. The following models were developed for the prediction of transverse cracking:

$$\begin{aligned}\text{CRACKSJP} = {} & \text{ESAL}^{2.755} * \left[3092.4 * (1 - \text{SOILCRS}) * \text{RATIO}^{10}\right] \\ & + \text{ESAL}^{0.5} * \left(1.233 * \text{TRANGE}^{2} * \text{RATIO}^{2.868}\right) \\ & + \text{ESAL}^{2.416} * \left(0.2296 * \text{FI}^{2.53} * \text{RATIO}^{7.31}\right)\end{aligned}$$

Statistics: $R^2 = .69$, SEE $= 176$, $N = 303$ (1)

$$\begin{aligned}\text{CRACKSJR} = {} & \text{ESAL}^{0.897} * \left[7130 * \text{JTSPACE}/\right. \\ & \left.(\text{ASTEEL} * \text{THICK}^{5})\right] + \text{ESAL}^{0.4} * \left(2.281 * \text{PUMP}^{5}\right) \\ & + \text{ESAL}^{2.16}\left[\frac{1.81}{(\text{BASETYP} + 1)}\right] \\ & + \text{AGE}^{1.1} * \left[0.0036 * (\text{FI} + 1)^{0.36}\right]\end{aligned}$$

Statistics: $R^2 = .41$, SEE $= 280$, $N = 314$ (2)

H.-W. Ker, Department of International Trade, Chihlee Institute of Technology, #313, Section 1, Wen-Hwa Road, Pan-Chiao, Taipei, Taiwan 220. Y.-H. Lee, E732, and C.-H. Lin, E801, Department of Civil Engineering, Tamkang University, #151 Ying-Chuan Road, Tamsui, Taipei, Taiwan 251. Corresponding author: Y.-H. Lee, yinghaur@mail.tku.edu.tw.

Transportation Research Record: Journal of the Transportation Research Board, No. 2068, Transportation Research Board of the National Academies, Washington, D.C., 2008, pp. 20–31.
DOI: 10.3141/2068-03

where

CRACKSJP = total length of transverse cracking, including low, medium, and high severities (ft/mi);
ESAL = accumulated 18-kip ESALs ($\times 10^6$);
SOILCRS = subgrade classification (1 for A1 to A3 coarse-grained soils, 0 for A4 to A7 fine-grained soils);
TRANGE = yearly temperature range (°F);
RATIO = stress ratio defined as the ratio of Westergaard edge stress versus concrete modulus of rupture;
FI = freeze index (°F-days);
CRACKSJR = sum of medium- and high-severity transverse cracking (ft/mi);
JTSPACE = mean transverse joint spacing (ft);
ASTEEL = cross area of reinforcing steels (in.²/ft of width);
THICK = slab thickness (in.);
PUMP = pumping status (0 for no pumping; 1, 2, and 3 for low-, medium-, and high-severity pumping, respectively);
BASETYP = base types (0 for granular base, 1 for treated base);
AGE = pavement age (years);
R^2 = coefficient of determination;
SEE = standard error of estimates; and
N = number of observations.

For the calculation of Westergaard edge stress, a single wheel load of 9,000 lb (40 kN), a concrete modulus of elasticity of 4.2 Mpsi (28.9 GPa), a Poisson ratio of 0.2, and a load radius of 6.4 in. (16.36 cm) were used. For JPCP model, the increase of slab thickness will result in stress reduction and thus significantly reduce the occurrence of transverse cracking. Sensitivity analysis also indicates that if the concrete modulus of rupture is below 600 psi (4.13 MPa) the stress ratio becomes higher, which will result in more transverse cracking. With better drainage in coarse-grained soil or base type, the possibility of pumping and loss of support are reduced and so is the occurrence of transverse cracking.

However, a field-collected pavement database may not contain a wide range of design parameters, and this situation may limit the inference space and the results of data interpretation. To remedy this problem, the LTPP program, since 1987, has been collecting a national pavement database in a factorial format with wider ranges of pavement designs, materials, and climatic zones. More than 2,400 asphalt and portland cement concrete pavement test sections across North America have been monitored. Detailed information about original construction, pavement inventory data, materials and testing, historical traffic counts, performance data, maintenance and rehabilitation records, and climatic information have been collected. In NCHRP Project P-393 (2), an early sensitivity analysis study of the LTPP database was conducted, and the following models were developed for the prediction of transverse cracking:

$$\mathrm{PCRACKED} = \frac{1}{0.01 + 10 * 100^{\log_{10}\mathrm{FD}}}$$

$$\mathrm{FD} = \sum_{i=1}^{k}\left(\frac{n_i}{N_{ti}}\right)$$

$$N_t = 10^{\left[2.13 * (1/\mathrm{RATIO})^{1.2}\right]} \qquad (3)$$

$$\mathrm{CRACKSJR} = -72.9 + 1.9 * \mathrm{ESAL} + 0.182\left(\frac{1}{\mathrm{PSTEEL}^2}\right) + 2473 * \left(\frac{1}{\mathrm{KSTATIC}}\right) + 0.697 * \mathrm{PRECIP}$$

Statistics: $R^2 = .48$, SEE = 20.8, $N = 27$ (4)

where

PCRACKED = percentage of slabs with transverse cracking for JPCP pavements,
FD = estimated cumulative fatigue damage,
k = number of axle load types,
n_i = expected number of load repetitions under different axle load types,
N_{ti} = corresponding maximum allowable number of repetitions,
CRACKSJR = number of medium- and high-severity transverse cracking (number/mi),
PSTEEL = percentage of longitudinal reinforcing steel,
PRECIP = average annual precipitations (in.), and
KSTATIC = modulus of subgrade reaction (psi/in.).

Westergaard edge stress and curling stress equations (8) were used to account for the combination effects of loading and thermal curling. The assumed temperature gradients in different climatic zones and slab thicknesses could be found elsewhere (2). A single wheel load of 9,000 lb (40 kN) and a coefficient of thermal expansion for the slab of 5.5×10^{-6}/°F were used in the analysis. Cumulative fatigue damage is determined by summing the damage caused by each load application on the basis of Miner's hypothesis accordingly. Slab thickness and the modulus of rupture are important factors affecting the calculation of fatigue damage and estimation of transverse cracking. Sensitivity analysis also indicated that a lower modulus of subgrade reaction or a lower percentage of reinforcing steel would result in higher deflection, larger crack width, and thus more transverse cracking for JRCP pavements. Similar conclusions may be achieved for pavements with higher traffic and precipitations as well.

In the recommended MEPDG (4), both bottom-up and top-down cracking are considered for the prediction of JPCP transverse cracking. No prediction model was proposed for JRCP pavements. The fatigue-cracking damage for JPCP is determined in an incremental manner on the basis of the more-complicated concept of axle load spectra (ALS). Various artificial neural network models were developed from the ISLAB2000 finite element model to compute critical stresses and deflections. Monthly damage was computed for different axle loads, load positions, and equivalent temperature differences over the analysis period. Traffic data were further processed to determine the equivalent number of single, tandem, and tridem axles. Hourly pavement temperature profiles generated from the enhanced integrated climate model were converted to monthly equivalent linear temperature differences. Monthly relative humidity data were used to account for the effects of seasonal changes in moisture conditions on differential shrinkage and were also converted to effective temperature difference. The proposed model is briefly summarized as follows:

$$\mathrm{PCRACKED} = \frac{1}{1 + \mathrm{FD}^{-1.68}}$$

$$\mathrm{FD} = \sum \frac{n_{i,j,k,l,m,n}}{N_{i,j,k,l,m,n}}$$

Statistics: $R^2 = .75$, SEE = 6.9, $N = 516$ (5)

where

$n_{i,j,k,l,m,n}$ = applied number of axle loads under each condition defined by subscripts;
i = age to account for change in modulus of rupture, layer bond condition, and deterioration of shoulder load transfer efficiency;
j = month to account for change in base and effective dynamic modulus of subgrade reaction;
k = axle type (single, tandem, and tridem for bottom-up cracking; short, medium, and long wheelbase for top-down cracking);
l = load level for each axle type;
m = temperature difference;
n = traffic path; and
$N_{i,j,k,l,m,n}$ = corresponding allowable number of load applications determined by the following field calibrated fatigue mode.

$$\log(N_{i,j,k,l,m,n}) = 2.0 * \left(\frac{MR_i}{\sigma_{i,j,k,l,m,n}} \right)^{1.22} + 0.4371 \qquad (6)$$

where MR_i equals the PCC modulus of rupture (psi) at age I and $\sigma_{i,j,k,l,m,n}$ equals the estimated stress (psi) at each condition.

DATABASE PREPARATION

Initially, the DataPave 3.0 program was used to prepare a database for this study. However, to obtain additional variables and the latest updates of the data, the LTPP database retrieved from www.datapave.com (or LTPP DataPave online, standard release 18.0) (*6*) became the main source for this study. There are eight general pavement studies (GPSs) and nine specific pavement studies (SPSs) in the LTPP program, of which only JPCPs (GPS3) and JRCPs (GPS4) were used for here. The database was implemented in an information management system (IMS) that is a relational database structure that uses the ORACLE program. However, the standard releases were in the Microsoft Access database structure. Automatic summary reports of the pavement information may be generated from different IMS modules, tables, and data elements.

The thickness of pavement layers was obtained from the IMS testing module rather than the IMS inventory module to be consistent with the results of the section presentation module in the DataPave 3.0 program. Several other material properties, such as the modulus of rupture, plasticity index, and the percent passing a No. 4 sieve, were queried from the inventory module. Detailed traffic counts and ESALs were obtained from the traffic module. The cumulated ESAL during the performance analysis period was calculated by multiplying pavement age with mean yearly ESAL (or kesalpyr), which could be easily estimated from the database. Environmental data were retrieved from the IMS climate module and the associated virtual weather station link.

There are distinct differences in the distress data collected from the two collection methods, that is, the manual survey (MON_DIS_JPCC_REV) and the photographic survey (MON_DIS_PADIAS42 JPCC) (*9*). Although techniques in collecting and interpreting LTPP photographic distress data may have been improved (*10*), for simplicity and consistency, only manual survey data were used in this study. The transverse-cracking data (low, medium, and high severities for JPCP and medium and high severities for JRCP) were obtained from the MON_DIS_JPCC_REV table in the IMS monitoring module. Maintenance and rehabilitation activities could effectively reduce the distress quantities. Thus, the records in both the maintenance and rehabilitation modules were used to assure that this study chose only the performance data of those sections without or before major improvements. For the purpose of this study, a Microsoft Excel summary table containing the pavement inventory, material and testing, traffic, climatic, and distress data was created by using the relational database features of the Access program. The Excel table was then stored as S-Plus data sets (*11*) for subsequent analysis. The summary, table, cor, plot, pairs, and coplot functions were heavily used to summarize the information of interest and to provide more reliable data for this study.

A data-cleaning process had to be conducted before any preliminary analysis or regression analysis could be performed. With the help of graphical representation, transverse-cracking data were plotted against surveyed years for each section in the database, with additional information displayed. For example, the plot shown in Figure 1 was used to examine the distress trends to identify possible data errors. The state code, SHRP identification number, modulus of rupture (MPa), slab thickness (cm), construction year, and mean yearly ESAL were labeled on each plot. Each section was carefully examined. Two additional codes were assigned to each section to indicate the findings of the examination (i.e., whether the transverse cracking was reasonable in relation to the distress history, or which year of data was questionable and could be deleted if necessary). For example, a comparison of the first three data points of pavement Section 6/3005 with the remaining data found that this section probably had some maintenance or rehabilitation activities, although they were not recorded in the database. Data correction and preparation were made in a way that could be easily traced. By doing so, different subsets of the final database providing more reliable data might be analyzed for different purposes.

COMPARISON OF LABORATORY-TESTED AND BACKCALCULATED MODULI

The modulus of each pavement layer, backcalculated by using the ERESBACK 2.2 program (*12*), was retrieved from the IMS monitoring module. The laboratory-tested layer moduli were compared with the backcalculated moduli so as to obtain a better understanding of their associated variability in the study. The variability of the relationship between the laboratory-tested (or static) and backcalculated (or dynamic) moduli could not be ignored. Figures 2*a* through 2*c* depict that the average ratios are approximately 1.4, 1.5, and 1.5 for surface, subbase, and subgrade layers, respectively, for a dense liquid foundation. Few laboratory-tested modulus of subgrade reactions were available in the database. Likewise, Figures 2*d* through 2*f* depict that the average ratios were roughly 1.0, 1.1, and 3.0 for surface, subbase, and subgrade layers, respectively, for an elastic solid foundation (*7*). For consistency, the recommendation by AASHTO (*13*) of dividing the backcalculated modulus of subgrade reaction (k-value, MPa/m) by 2 as the static k-value was used in the calculation of the stress ratio in this study.

RELATIONSHIP BETWEEN ELASTIC MODULUS AND MODULUS OF SUBGRADE REACTION

For practical reasons, a relationship between the elastic modulus and the modulus of subgrade reaction is often needed. According to the literature (*12*), the following empirical relationship was developed from the GPS and SPS data analysis:

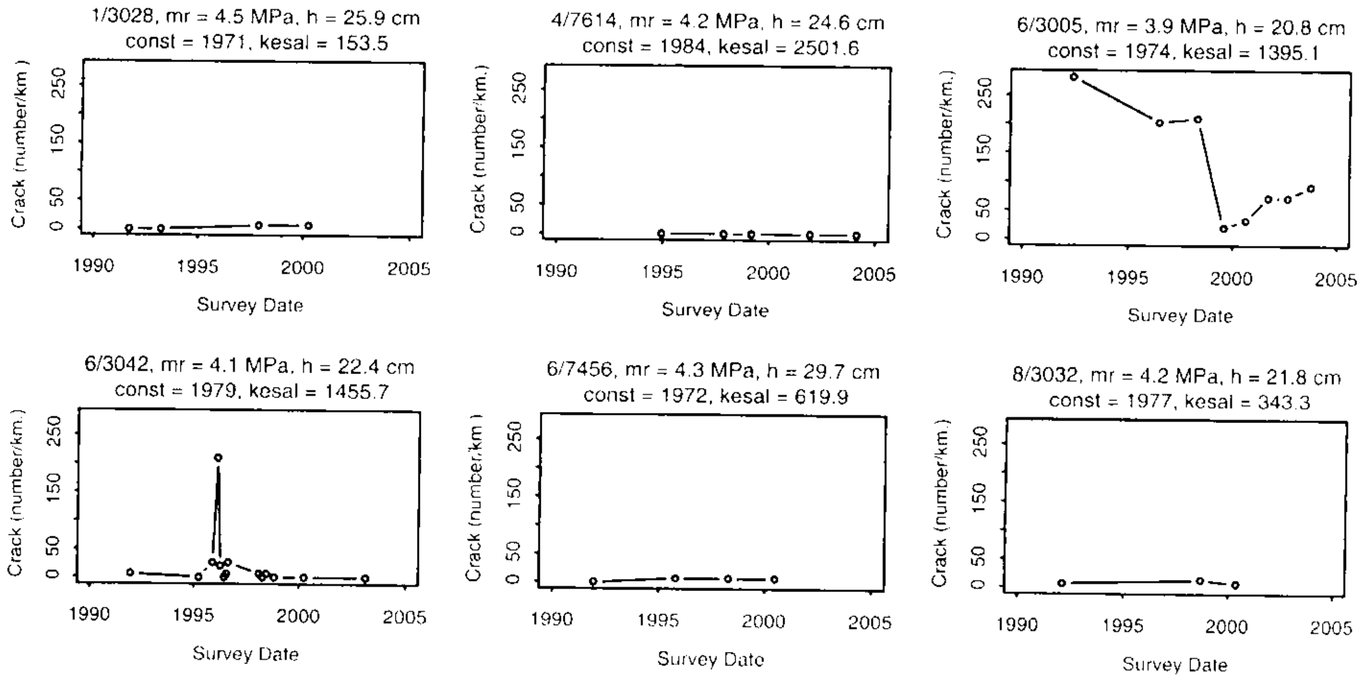

FIGURE 1 Some transverse-cracking history of JPCP pavements.

$$k = 0.296E_s$$

Statistics: $R^2 = .872$, SEE = 9.37, $N = 596$ (7)

where k is the modulus of subgrade reaction (MPA/m) and E_s is the subgrade elastic modulus (MPa). According to the available GPS data, very good agreements have been achieved with the above relationship.

Nevertheless, Barenberg (*14*) indicated a theoretical difference by using an elastic solid foundation and a dense liquid foundation having the same maximum deflections in backcalculation analysis. Assuming a Poisson ratio of 0.5 for the subgrade, a Poisson ratio of 0.15 for the concrete slab, and an elastic modulus for the slab of 4 Mpsi (27.6 GPa), the following relationship was derived after a simplification process:

$$E_s = 283.7 * h * k \qquad (8)$$

where

k = modulus of subgrade reaction ($lb/in.^3$),
E_s = subgrade elastic modulus (psi), and
h = slab thickness (in.).

As Figure 3*a* shows, the effect of slab thickness has to be considered in such a relationship.

The aforementioned relationship was further verified with a comparison of the backcalculated subgrade elastic moduli with the backcalculated modulus of subgrade reaction from the LTPP database. Slab thickness had significant effects on this relationship, as shown in Figure 3*b*. Consequently, the following relationship was developed by using regression techniques:

$$E_s = 0.9015(k * h)$$

Statistics: $R^2 = .9524$, SEE = 15.87, $N = 138$ (9)

where

k = modulus of subgrade reaction (MPa/m),
E_s = subgrade elastic modulus (MPa), and
h = slab thickness (cm).

PRELIMINARY ANALYSIS OF TRANSVERSE-CRACKING DATABASE

Univariate Data Analysis

Univariate data analysis consists of statistical methods for describing the distribution and spread of each variable. Some basic descriptive statistics of JPCP pavements about the data range, its variation, and the number of observations for each variable are given in Tables 1 and 2. The univariate data analysis procedure is often used to investigate the possibility of data errors and potential distribution problems for each variable considered in a regression analysis. A few extreme (or unusual) data points may be identified or deleted from the analysis (as, for example, in the bottom half of Table 2). In the tables, age stands for pavement age (years); kesalpyr is the yearly ESALs (thousands); cesal is the cumulative ESALs (millions); jtspace is the transverse joint spacing (m); hpcc is the slab thickness (cm); fi is yearly freezing index (°C-days); precip is the mean annual precipitation (mm); kstatic is the modulus of subgrade reaction (MPa/m); trange is the difference between the maximum and the minimum mean annual temperature (°C); days32 is the number of days the temperature was above 32°C; ft is the yearly freeze–thaw cycle; mr is the concrete modulus of rupture (MPa); ratio is the stress ratio; and act.crack is the percentage of cracked slabs (%).

A graph is always far more perceptible than thousands of numbers. A single plot that well describes the spread of the data may be created by combining these univariate statistics with a histogram. A simplified distribution plot that graphically displays the variability of

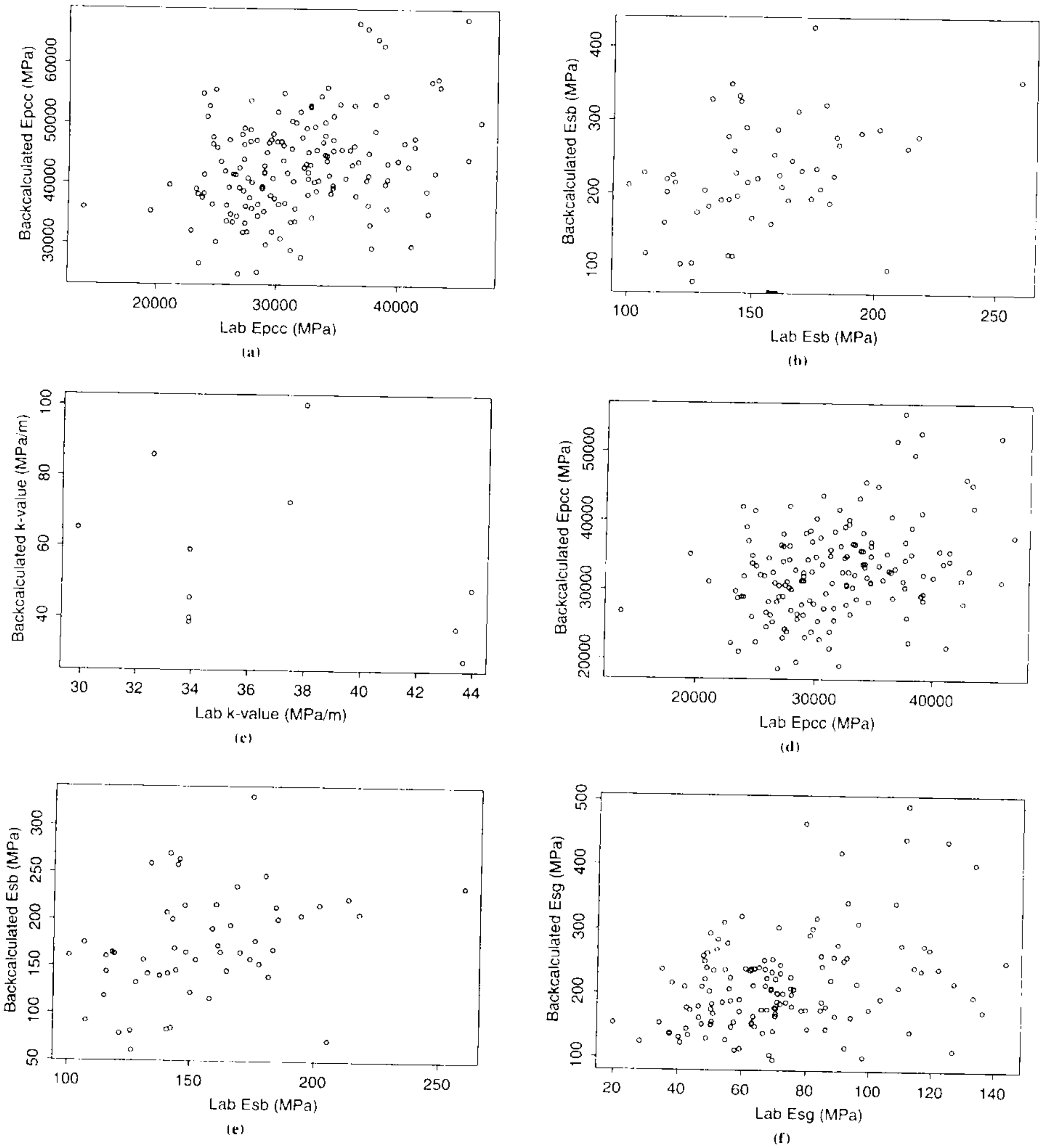

FIGURE 2 Comparison of laboratory-tested and backcalculated layer moduli of (a) surface, (b) subbase, and (c) subgrade for dense liquid foundation and of (d) surface, (e) subbase, and (f) subgrade for elastic solid foundation, respectively.

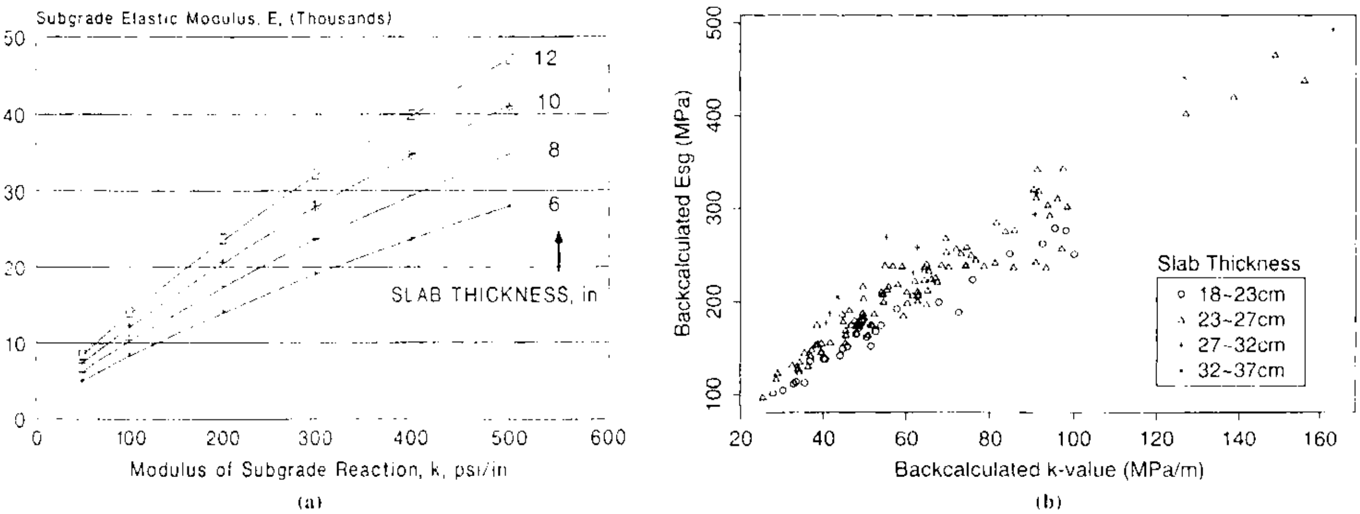

FIGURE 3 **Comparison of elastic solid foundation versus dense liquid foundation: (*a*) theoretical comparison (*14*) and (*b*) backcalculated results.**

data, including median, lower and upper quantiles, 95% confidence intervals, and extreme points (if any) may be made in a box plot. A box plot displays not only the location and spread of the data but also skewness. A histogram displays only a rough and crude shape of the distribution of data. To have a smoother look, a continuous curve of the nonparametric estimate of the probability density may also be obtained. A normal probability plot or a quantile–quantile plot can be used to provide a quick visual check on the assumption of a normal distribution. If the distribution is close to normal, the plot will show approximately a straight-line relationship. The distribution of transverse cracking (act.crack) of JPCP pavements is shown in Figure 4. The solid horizontal line in the box plot indicates the median of the data, whereas the upper and lower ends of the box show the upper and lower quantiles, respectively. These plots reveal a relatively skewed distribution for actual transverse cracking.

Bivariate and Multivariate Analysis

A correlation matrix of these variables is also given in Table 2. In addition, trimmed correlation matrices show the variable correlations after a certain portion of influential data points or possible outliers are eliminated (3% in this example) such that more reliable indices of the correlations are obtained. The difference between the resulting traditional correlation matrix and the trimmed correlation matrix is shown in Table 2. A scatter plot matrix can graphically represent their relationships and scatters. With the application of a data-smoothing technique (lowess) on the same scatter plot matrix, the pairwise relationships as shown in Figure 5 become clearer, and possible data errors may be identified. In Figure 5, age, cesal, trange, and ft have better correlations with actual transverse cracking (act.crack) although high variations are still observable.

TABLE 1 **Univariate Statistics**

	N	Mean	Std. Dev.	Sum	Min.	Max.
age	393	16.44	6.34	6,460.90	2.34	35.64
kesalpyr	393	485.72	433.73	190,886.02	20.21	2,501.62
cesal	393	7.83	7.45	3,077.23	0.16	33.90
jtspace	393	5.02	0.83	1,972.18	3.51	6.55
hpcc	393	24.22	2.97	9,518.14	16.26	36.32
fi	393	246.92	367.12	97,039.23	0.00	1,777.22
precip	393	883.58	428.66	347,248.12	118.71	1,725.67
kstatic	393	33.80	14.79	13,281.69	12.75	81.58
trange	393	12.87	2.08	5,058.77	8.40	18.04
days32	393	43.88	31.41	17,245.62	0.15	174.35
ft	393	68.31	44.00	26,846.65	0.00	173.13
mr	393	4.46	0.41	1,754.72	3.03	5.88
ratio	393	0.44	0.10	173.40	0.21	0.77
act.crack	393	5.71	16.22	2,242.50	0.00	100.00

TABLE 2 Multiple Correlations of JPCP Pavements

	age	cesal	jtspace	hpcc	fi	precip	kstatic	trange	ft	mr	ratio	act.crack
Correlation Matrix												
age	1.00	0.26	0.16	−0.13	−0.10	0.13	−0.18	−0.17	−0.11	−0.14	0.17	0.16
cesal	0.26	1.00	0.02	0.17	−0.27	0.17	0.06	0.37	−0.13	−0.12	−0.20	0.33
jtspace	0.16	0.02	1.00	0.02	−0.18	0.68	0.20	−0.21	−0.18	−0.10	−0.09	0.01
hpcc	−0.13	0.17	0.02	1.00	−0.07	−0.01	0.16	0.01	0.00	0.00	−0.86	−0.02
fi	−0.10	−0.27	−0.18	0.07	1.00	−0.27	0.24	−0.16	0.46	0.07	0.21	−0.06
precip	0.13	−0.17	0.68	−0.01	−0.27	1.00	0.20	−0.58	0.40	0.01	−0.02	−0.02
kstatic	0.18	0.06	0.20	0.16	0.24	0.20	1.00	0.02	−0.13	0.09	−0.37	0.03
trange	−0.17	0.37	−0.21	0.01	−0.16	−0.58	0.02	1.00	0.36	0.02	−0.10	0.20
ft	0.11	0.13	−0.18	0.00	0.46	−0.40	0.13	0.36	1.00	0.04	0.00	0.19
mr	0.14	0.12	−0.10	0.00	0.07	0.01	0.09	0.02	0.04	1.00	−0.38	−0.03
ratio	0.17	−0.20	−0.09	−0.86	0.21	−0.02	0.37	−0.10	0.00	0.38	1.00	0.00
act.crack	0.16	0.33	0.01	−0.02	−0.06	−0.02	0.03	0.20	0.19	−0.03	0.00	1.00
Trimmed Correlation Matrix (deleted 3% of data)												
age	1.00	0.30	0.20	−0.11	0.05	0.16	−0.18	−0.17	−0.13	−0.16	0.19	0.18
cesal	0.30	1.00	0.04	0.26	−0.15	−0.18	0.11	0.43	−0.14	0.08	−0.25	0.30
jtspace	0.20	0.04	1.00	0.05	0.14	0.71	0.22	0.19	−0.16	0.16	−0.09	0.02
hpcc	0.11	0.26	0.05	1.00	−0.04	0.05	0.21	0.10	0.04	0.09	0.88	0.08
fi	0.05	−0.15	−0.14	−0.04	1.00	0.27	−0.15	0.13	0.60	0.10	0.15	0.18
precip	0.16	−0.18	0.71	0.05	−0.27	1.00	0.18	−0.60	−0.42	−0.13	0.05	−0.08
kstatic	−0.18	0.11	0.22	0.21	−0.15	0.18	1.00	0.11	−0.10	0.17	−0.38	0.14
trange	0.17	0.43	0.19	0.10	−0.13	0.60	0.11	1.00	0.39	0.06	−0.15	0.17
ft	−0.13	−0.14	−0.16	0.04	0.60	−0.42	−0.10	0.39	1.00	0.17	−0.05	0.16
mr	0.16	−0.08	−0.16	0.09	0.10	−0.13	0.17	0.06	0.17	1.00	−0.38	0.19
ratio	0.19	−0.25	−0.09	−0.88	0.15	0.05	−0.38	−0.15	−0.05	0.38	1.0	−0.03
act.crack	0.18	0.30	0.02	0.08	0.18	0.08	0.14	0.17	0.16	0.19	0.03	1.00

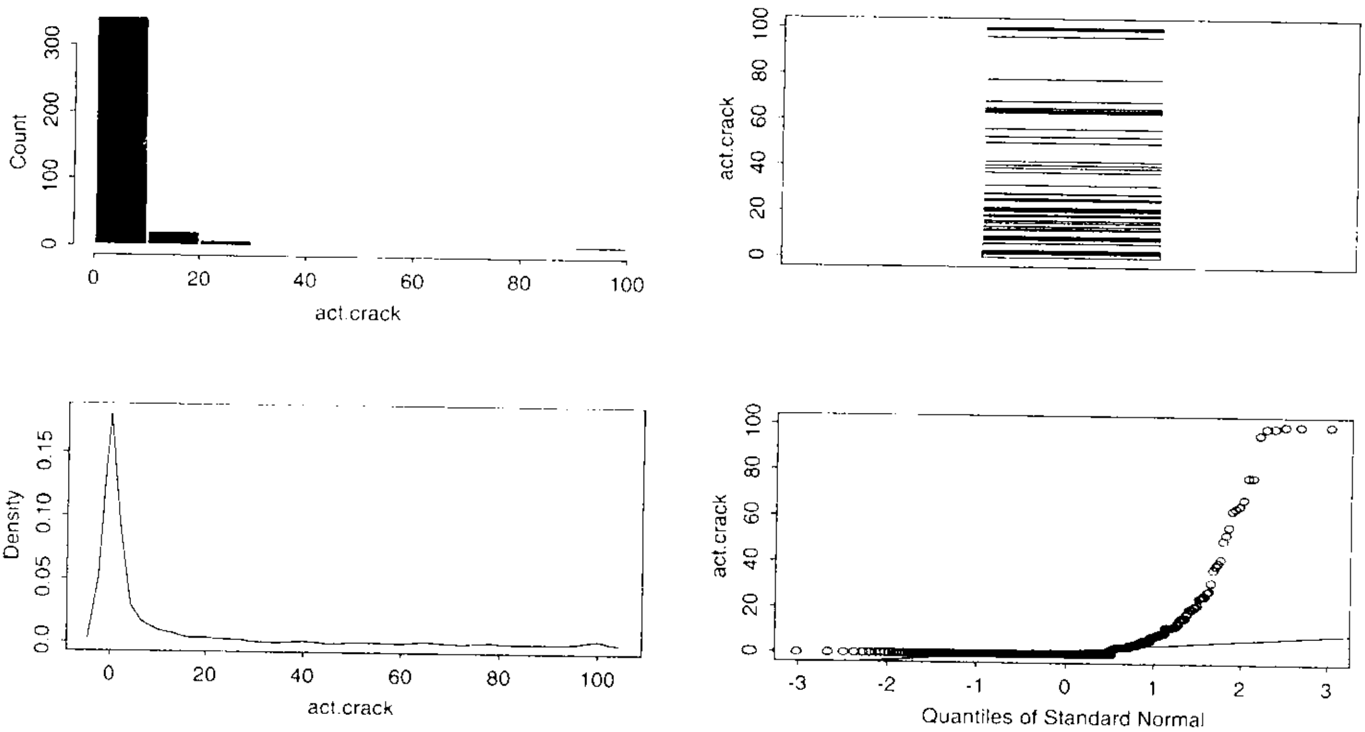

FIGURE 4 Exploratory data analysis: transverse cracking of JPCP pavements.

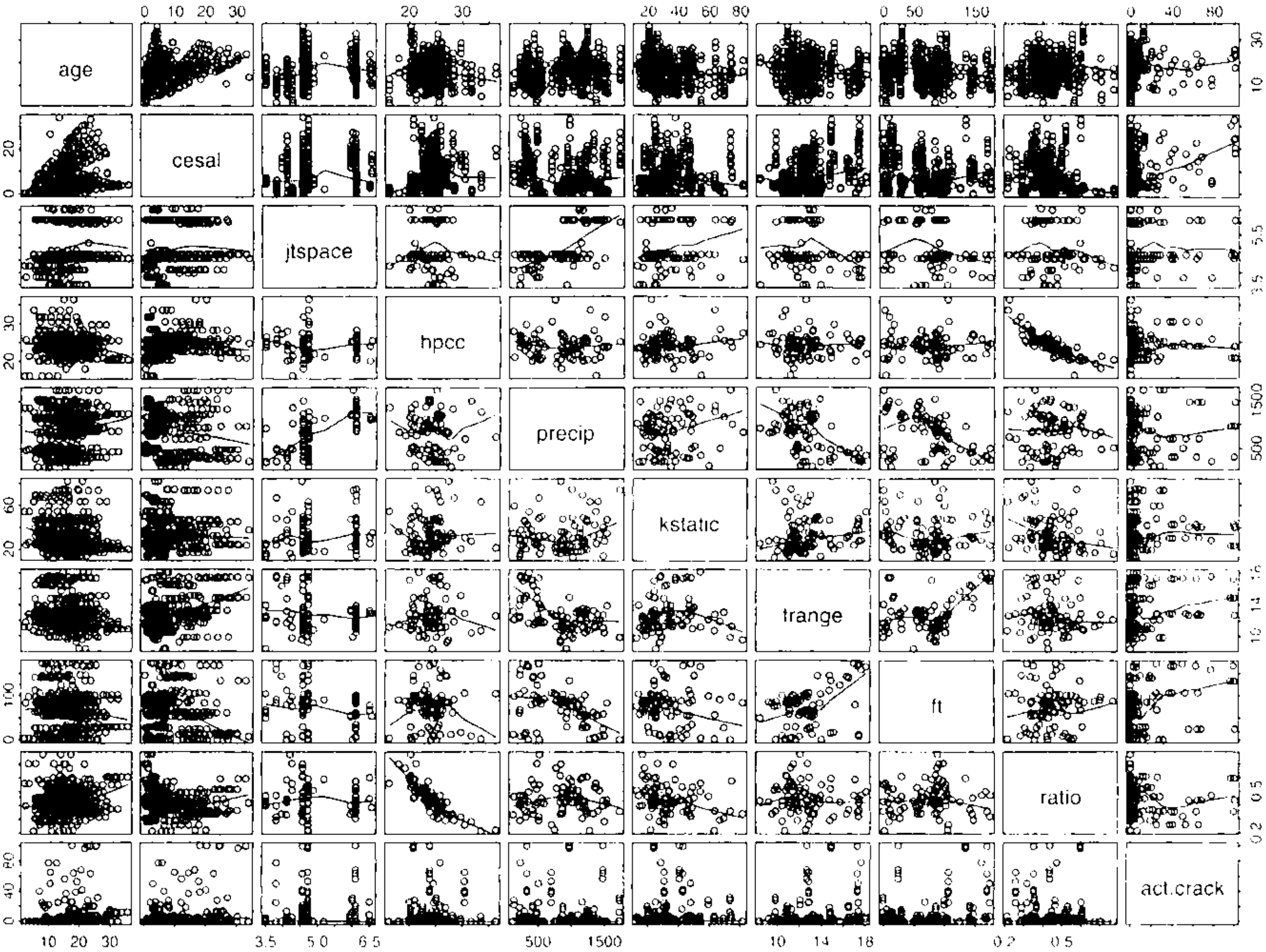

FIGURE 5 Use of smoother (lowess) on the scatter plot matrix for JPCP pavements.

The slab thickness (hpcc) is highly correlated with stress ratio (ratio), and transverse joint spacing (jtspace) is also highly correlated with annual precipitation (precip). Special cautions are needed during the modeling process to avoid potential collinearity problems.

INVESTIGATION OF GOODNESS OF FIT OF EXISTING MODELS

To investigate the goodness of predictions, the models given in Equations 1 to 4 were used to predict the occurrence of transverse cracking, and the results were plotted against the actual observed data. Figures 6*a* and 6*b* show the goodness of prediction with NCHRP 1-19 models for JPCP and JRCP pavements, respectively. Similarly, Figures 6*c* and 6*d* depict the results of this comparison with P-393 models for JPCP and JRCP pavements, respectively. Visual graphical techniques such as condition plots were used to assist in the identification of the factors affecting the goodness of predictions. For example, it was found that the circled data with relatively high predictions in Figure 6*d* resulted from the very small longitudinal reinforcement.

The prediction accuracy of the proposed models implemented in the recommended MEPDG (*4*) was further investigated. To avoid undesirable misunderstanding of the new guide's prediction algorithm due to the complexity involved, direct use of the MEPDG software was chosen for prediction of transverse cracking. The beta version of the software was downloaded from www.trb.org/mepdg/software.htm. A total of 22 JPCP pavement sections containing 102 data points were randomly selected for this analysis. The goodness of transverse-cracking prediction with NCHRP Project P-393 models and the recommended MEPDG (DG2002) models are shown in Figures 6*e* and 6*f*. Apparently, the prediction accuracy of the existing models was found to be inadequate.

DEVELOPMENT OF IMPROVED TRANSVERSE-CRACKING MODELS

The occurrence of transverse cracking in the field depends on various factors, namely traffic, environment, structure, construction, maintenance, and rehabilitation. Even though the use of cumulative fatigue damage based on Miner's hypothesis and the more-complicated ALS concept seems to be a logical approach, their integration with monthly or seasonal environmental factors (such as humidity and temperature differentials) often resulted in more variations in the predictions of transverse cracking, as shown in Figures 6*c*, 6*e*, and 6*f*, due to the many uncertainties involved.

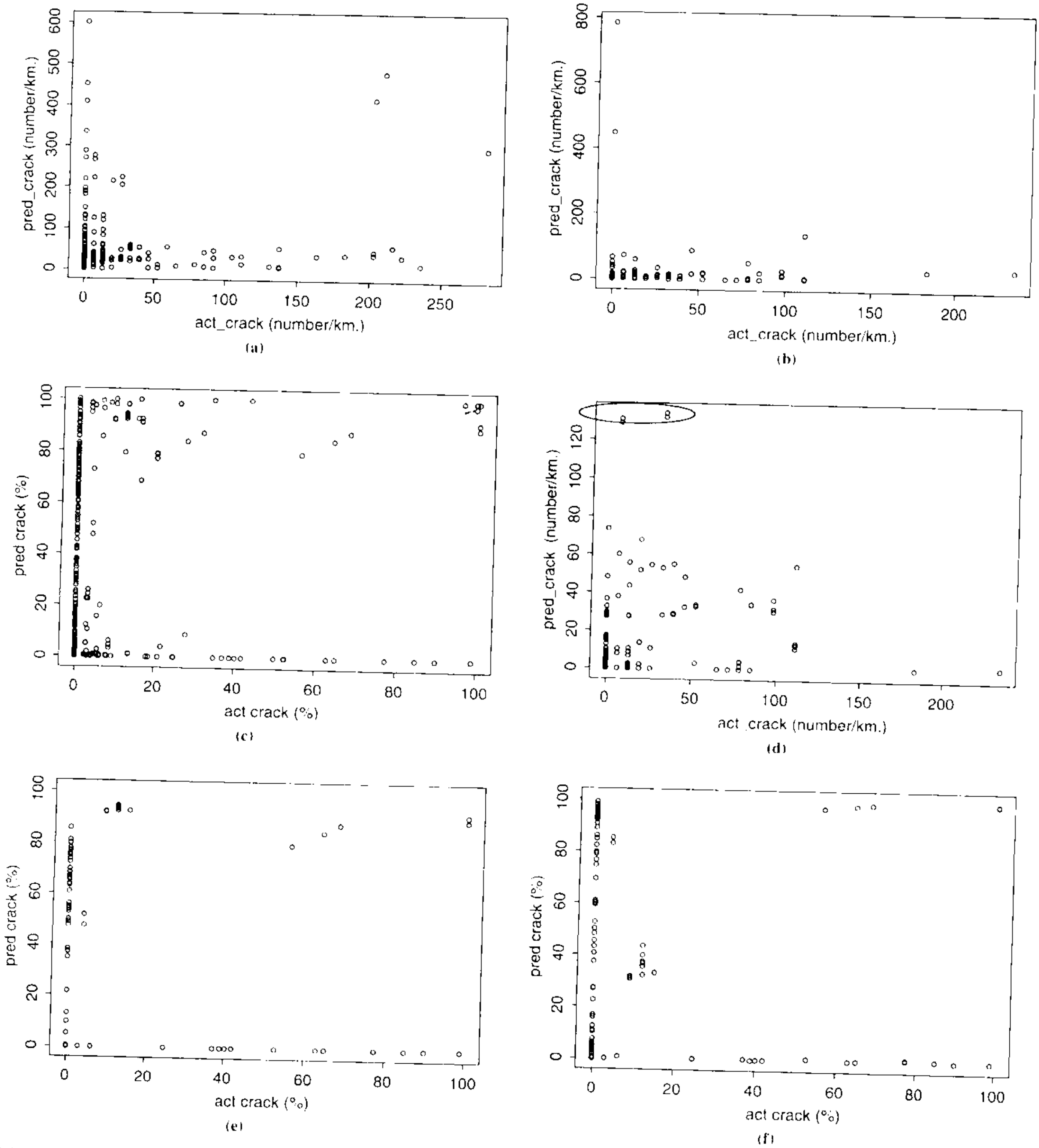

FIGURE 6 Comparison of prediction results by using *(a)* NCHRP 1-19 JPCP, *(b)* NCHRP 1-19 JRCP, *(c)* P-393 JPCP, *(d)* P-393 JRCP, *(e)* P-393 JPCP, and *(f)* DG2002 models.

To develop a more-reliable predictive model for practical engineering problems, Lee and Darter (*15, 16*) proposed a predictive modeling approach to incorporate robust (least median squared) regression, alternating conditional expectations, and additivity and variance-stabilization algorithms into the modeling process. The robust regression was proposed because of its favorable feature of analyzing highly contaminated data by detecting outliers from both the dependent variable and independent variables. Through the iterative use of the combination of these outlier detection and nonparametric transformation techniques, it was believed that some potential outliers and proper functional forms might be identified. Subsequently, traditional regression techniques can be easily used for model development. Nevertheless, it has been extremely difficult to achieve a satisfactory predictive model for this set of data by using these regression techniques in many preliminary trials.

Exploratory data analysis of the response variable as shown in Figure 4 has indicated that the normality assumption with random errors and constant variance by using conventional regression techniques might not be appropriate for prediction modeling. The distribution of transverse cracking was tested for departures from normality by using Shapiro and Wilk's W-statistic (*11*). Various transformations, including the logarithm of the transverse cracking, were tested, although the W-statistic still indicated that transverse cracking did not have a lognormal distribution, either. Because of the nature of collecting data on transverse cracking, those data could be treated as rate data (i.e., percentage of cracked slab). Agresti suggested that "when events of a certain type occur over time, space, or some other index of size, it is often relevant to model the rate at which events occur," and using the Poisson regression for rate data is an appropriate decision (*17*, p. 86).

Preliminary Analysis Using Poisson Regression Techniques

Therefore, the generalized linear model (GLM) (*18*), along with the assumption of Poisson distribution, was adopted in this analysis. Here, a Poisson log-linear model is a GLM that assumes a Poisson distribution for the response variable and uses the log link. Many factors, including age, kesalpyr, cesal, jtspace, hpcc, fi, precip, kstatic, trange, days32, ft, basetype [base types (0 for granular base, 1 for treated base)], stype [subgrade types (1 for A1 to A3 coarse-grained soil, 0 for A4 to A7 fine-grained soil)], edgestress [estimated Westergaard edge stress (MPa)], mr, ratio, and psteel were considered in the beginning trial analysis (with those variables not defined here having their earlier definitions). After several attempts to eliminate parameters that were, from both statistical and engineering viewpoints, insignificant or inappropriate, the following models were obtained:

$$\begin{aligned}\ln(\text{PCRACKED}) = {} & -6.105 + 0.1015 * \text{age} + 0.001317 * \text{kesalpyr} \\ & + 0.001209 * \text{precip} + 0.01284 * \text{ft} \\ & + 0.1999 * \text{trange} + 1.031 * \text{ratio}\end{aligned}$$

Statistics: $N = 393$, null deviance $= 8{,}138.5$,
residual deviance $= 5{,}402.1$ (10)

$$\begin{aligned}\ln(\text{CRACKSJR}) = {} & -0.9396 + 0.06729 * \text{cesal} + 0.02152 * \text{ft} \\ & + 0.2326 * \text{trange} - 10.26 * \text{psteel}\end{aligned}$$

Statistics: $N = 151$, null deviance $= 5{,}391.9$,
residual deviance $= 2{,}991.3$ (11)

where PCRACKED is the percentage of cracked slabs for JPCP pavements and CRACKSJR is the number of medium- and high-severity transverse cracks (number/km). The dispersion parameter for the Poisson family was taken to be 1. Here, a total of 74, 43, 114, and 162 data points were obtained from dry–freeze, dry–nonfreeze, wet–freeze, and wet–nonfreeze zones for JPCP pavements, whereas the performance data of JRCP pavements consisted of only 80 and 71 observations from wet–freeze and wet–nonfreeze zones, respectively.

The primary assumption of the above preliminary GLM models was that a linear function of the parameters was used in the model. The generalized additive model (GAM) extends GLM by fitting nonparametric functions by data-smoothing techniques to estimate the relationship between the response and the predictors (*19*). To further enhance the model fits, GAM techniques were adopted in this analysis. The Box–Cox power transformation technique was routinely used to estimate a proper monotonic transformation for each variable on the basis of the resulting preliminary GAM model. The transverse-cracking data were refitted with these transformed predictors with GLM techniques. Visual graphical techniques as well as the systematic statistical and engineering approach proposed by Lee and Darter (*15, 16*) were frequently adopted during the prediction-modeling process. A plot of residuals versus the fitted values could be used to check the adequacy of the model. If any curvature was observed, then the model could be improved by adding more nonlinear terms to the model.

After a considerable number of trials, the following models were separately developed for the transverse-cracking prediction of JPCP and JRCP pavements. As Figure 7 shows, a plot of the observed versus the fitted values illustrates the goodness of fit.

$$\text{PCRACKED} = \exp\left[\begin{aligned} & -9.913 + 3.711 * \log(\text{age}) + 1.931 \\ & * \log \text{kesalpyr} + 0.05116 * \sqrt{\text{precip}} + 0.01186 \\ & * \text{ft} - 26.71 * \frac{1}{\text{trange}} + 2.496 * \sqrt{\text{ratio}} \end{aligned}\right]$$

Statistics: $N = 393$, $R^2 = .358$, SEE $= 13.01$ (12)

$$\text{CRACKSJR} = \exp\left[\begin{aligned} & -5.863 - 1.780 * \frac{1}{\sqrt{\text{cesal}}} + 0.2397 \\ & * \sqrt{\text{ft}} - 37.25 * \frac{1}{\text{trange}} - 10.12 * \text{psteel} \end{aligned}\right]$$

Statistics: $N = 151$, $R^2 = .380$, SEE $= 20.79$ (13)

To improve the model fits further, it is possible to develop separate models for different climatic zones to account for other factors not considered implicitly in the above model. For example, the following two models could be subsequently developed by using the same functional forms with somewhat better regression statistics for JPCP pavements in the wet–nonfreeze zone and JRCP pavements in the wet–freeze zone, respectively. Nevertheless, it is still possible to develop better, more-refined models with more efforts in identifying other important factors and functional forms under different climatic conditions.

$$(\text{PCRACKED})_{\text{WNF}} = \exp\left[\begin{aligned} & -37.33 + 7.042 * \log(\text{age}) + 4.565 \\ & * \log \text{kesalpyr} + 0.2242 * \sqrt{\text{precip}} \\ & - 0.02321 * \text{ft} - 71.77 * \frac{1}{\text{trange}} \\ & + 24.77 * \sqrt{\text{ratio}} \end{aligned}\right]$$

Statistics: $N = 162$, $R^2 = .818$, SEE $= 8.26$ (14)

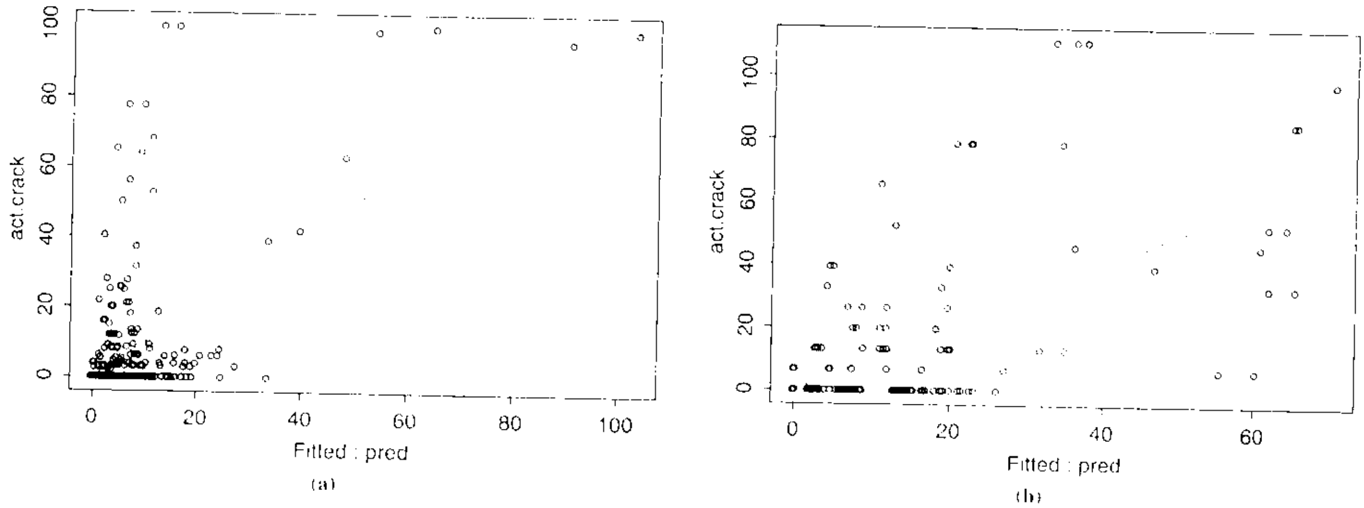

FIGURE 7 Goodness of fit of the proposed model for (*a*) JPCP and (*b*) JRCP pavements.

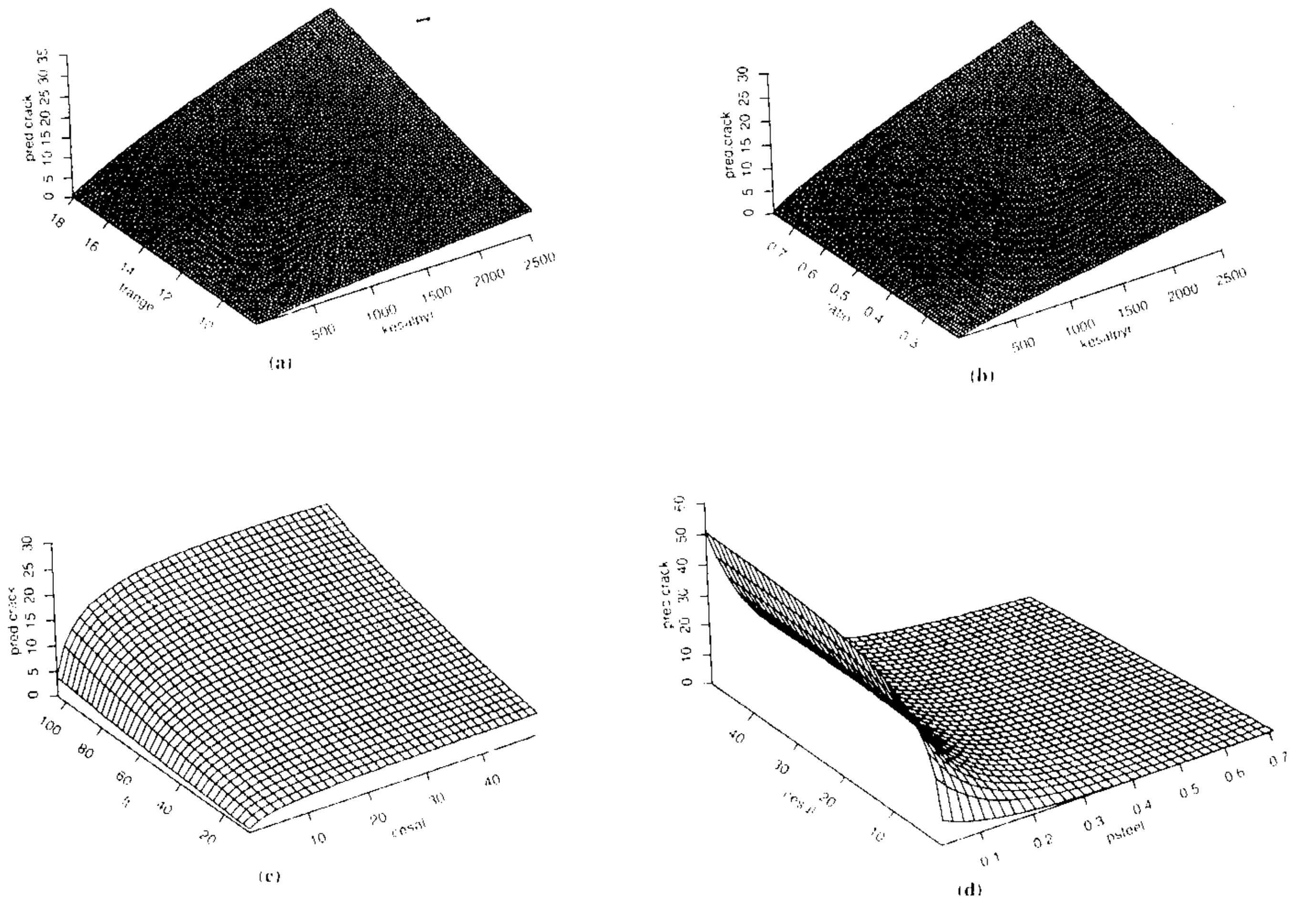

FIGURE 8 Sensitivity analysis of the proposed model for (*a*) and (*b*) JPCP and (*c*) and (*d*) JRCP.

$$(\text{CRACKSJR})_{WI} = \exp\left[\begin{array}{c} 7.142 - 1.927 * \frac{1}{\sqrt{\text{cesal}}} + 0.1459 \\ * \sqrt{\text{ft}} - 41.87 * \frac{1}{\text{trange}} - 8.500 * \text{psteel} \end{array}\right]$$

Statistics: $N = 80$, $R^2 = .393$, SEE = 23.95 (15)

Sensitivity Analysis of Tentatively Proposed Models

The goodness of the model fit was further examined through significant testing and various sensitivity analyses of pertinent explanatory parameters. Some plots showing the sensitivity of the various factors in the tentatively proposed models, that is, Equations 12 and 13, are presented in Figure 8. These plots were prepared on the basis of the range of the actual data while the remaining parameters were set to the corresponding mean values. The plots show the relationships among annual temperature range (trange), yearly ESALs (kesalpyr), stress ratio (ratio), pavement age (age) for the JPCP model, and yearly freeze–thaw cycle (ft), cumulated ESAL (cesal), and percent of reinforcing steel (psteel) for the JRCP model. The general trends of these effects seem to be fairly reasonable.

DISCUSSION AND CONCLUSIONS

Even though the use of cumulative fatigue damage based on Miner's hypothesis and the more-complicated ALS concept as recommended by the MEPDG seems to be a logical approach, integration of that information with monthly or seasonal environmental factors such as humidity and temperature differentials often resulted in more variations in the predictions of transverse cracking because of the many uncertainties involved. The prediction accuracy of the existing transverse-cracking models for jointed concrete pavements was found to be inadequate and greatly in need of improvement.

A relatively skewed distribution for actual transverse cracking was identified and also indicated that the normality assumption using conventional regression techniques might not be appropriate for this study. Thus, a GLM and a GAM along with the assumption of Poisson distribution were adopted for the modeling process. After many trials in eliminating insignificant and inappropriate parameters, the resulting proposed models included several variables (such as pavement age, yearly ESALs, cumulated ESALs, annual precipitation, freeze–thaw cycle, annual temperature range, stress ratio, and percent steel) for the prediction of transverse cracking.

The goodness of the model fit was further examined. The plot of the response versus fitted values indicated that the proposed model provided substantial improvements over the existing models. Sensitivity analysis of the explanatory variables indicated that their general trends seem to be fairly reasonable. The tentatively proposed predictive models appeared to agree reasonably with the pavement performance data, although their further enhancements are possible and recommended.

ACKNOWLEDGMENT

This study was sponsored by the National Science Council, Taiwan.

REFERENCES

1. Darter, M. I., J. M. Becker, and M. B. Snyder. *NCHRP Report No. 277: Portland Cement Concrete Pavement Evaluation System (COPES).* TRB, National Research Council, Washington, D.C., Sept. 1985.
2. Simpson, A. L., J. B. Rauhut, P. R. Jordahl, E. Owusu-Antwi, M. I. Darter, R. Ahmad, O. J. Pendleton, and Y.-H. Lee. *Early Analyses of LTPP General Pavement Studies Data, Volume 3: Sensitivity Analyses for Selected Pavement Distresses.* Report SHRP-P-393 SHRP, National Research Council, Washington, D.C., April 1994.
3. *Design and Construction of PCC Pavements, Volume III: Improving PCC Performance Models.* FHWA-RD-98-113, FHWA, U.S. Department of Transportation, Washington, D.C., 1999.
4. *Guide for Mechanistic-Empirical Design of New and Rehabilitated Pavement Structures.* NCHRP 1-37A, Transportation Research Board of the National Academies, Washington, D.C., 2004.
5. *Distress Identification Manual for the Long-Term Pavement Performance Program.* FHWA-RD-03-031, FHWA, U.S. Department of Transportation, 2003.
6. *Long-Term Pavement Performance Information Management System: Pavement Performance Database Users Reference Guide.* FHWA-RD-03-088, FHWA, U.S. Department of Transportation, 2004.
7. Lin, C.-H. *Development of Performance Prediction Models for Rigid Pavements Using LTPP Database* (in Chinese). Master's thesis, Tamkang University, Taiwan, 2007.
8. Huang, Y. H. *Pavement Analysis and Design,* 2nd ed. Prentice Hall, Upper Saddle River, N.J., 2004.
9. Daleiden, J. F., and A. L. Simpson. Evaluation of Strategic Highway Research Program—Long-Term Pavement Performance Surface Distress Data Collection Procedures. In *Transportation Research Record 1435,* TRB, National Research Council, Washington, D.C., 1994, pp. 8–15.
10. Rada, G. R., A. L. Simpson, and J. E. Hunt. Collecting and Interpreting Long-Term Pavement Performance Photographic Distress Data: Quality Control–Quality Assurance Processes. In *Transportation Research Record: Journal of the Transportation Research Board, No. 1889,* Transportation Research Board of the National Academies, Washington, D.C., 2004, pp. 97–105.
11. *S-Plus 6.2 for Windows: User's Manual, Language Reference.* Insightful Corp., Seattle, Wash., 2003.
12. *Backcalculation of Layer Parameters for LTPP Test Sections-Slab on Elastic Solid and Slab on Dense-Liquid Foundation Analysis of Rigid Pavements,* FHWA-RD-00-086, FHWA, U.S. Department of Transportation, Washington, D.C., 2001.
13. *AASHTO Guide for Design of Pavement Structures,* AASHTO, Washington, D.C., 1993.
14. Barenberg, E. J. Introduction to Concrete Pavement Design. *Proc., a Workshop on Modern Concrete Pavement Design,* Tamkang University, Taipei, Taiwan, May 3–4, 2000.
15. Lee, Y. H. *Development of Pavement Prediction Models.* Ph.D. dissertation. University of Illinois, Urbana, 1993.
16. Lee, Y.-H., and M. I. Darter. Development of Performance Prediction Models for Illinois Continuously Reinforced Concrete Pavements. In *Transportation Research Record 1505,* TRB, National Research Council, Washington, D.C., 1995, pp. 75–84.
17. Agresti, A. *An Introduction to Categorical Data Analysis.* John Wiley & Sons, Inc., New York, 1996.
18. Nelder, J. A., and R. W. M. Wedderburn. Generalized Linear Models. *Journal of the Royal Statistical Society, Series A,* Vol. 135, 1972, pp. 370–384.
19. Venables, W. N., and B. D. Ripley. *Modern Applied Statistics with S.* 4th ed. Springer-Verlag, New York, 2002.

The Pavement Monitoring, Evaluation, and Data Storage Committee sponsored publication of this paper.